doi:10.2533/chimia.2024.243 Chimia 78 (2024) 243–250

Oxidative Defect Detection Within Free and Packed DNA Systems: A Quantum Mechanical/Molecular Mechanics (QM/MM) Approach

Sophia Johnson[§] and Ursula Rothlisberger*

[§]SCS-dsm-firmenich Award for best poster presentation in Computational Chemistry

Abstract: Base excision repair enzymes (BERs) detect and repair oxidative DNA damage with efficacy despite the small size of the defects and their often only minor structural impact. A charge transfer (CT) model for rapid scanning of DNA stretches has been evoked to explain the high detection rate in the face of numerous, small lesions. The viability of CT DNA defect detection is explored *via* hybrid QM/MM computational studies that leverage the accuracy of quantum mechanics (QM) for a region of interest and the descriptive power of molecular mechanics (MM) for the remainder of the system. We find that the presence of an oxidative lesion lowers the redox free energy of oxidation by approximately 1.0 eV regardless of DNA compaction (free DNA versus packed DNA in nucleosome core particles) and damage location indicating the high feasibility of a CT-based process for defect detection in DNA.

Keywords: Chromatin · DNA · Molecular dynamics · Oxidative damage · QM/MM

Sophia Johnson completed her BSc in Chemistry from the University of Texas (UT) in 2012. She advised as a curriculum specialist at UT and trained teaching assistants. Later, she developed back-end taxonomies and supervised teams for the US market at Indeed, Inc. She returned to UT to direct the Inventors Program, a science entrepreneurship initiative. She began her PhD in 2021 under the supervision of Professor Ursula Rothlisberger of the Laboratory of Computational Chemistry and Biochemistry (LCBC) at Ecole Polytechnique Fédérale de Lausanne (EPFL) in Lausanne, Switzerland. Sophia investigates the mechanisms and properties of hormone-related DNA damage *via* multiscale computational techniques.

Ursula Rothlisberger is a full professor at EPFL in Lausanne, Switzerland serving as the principal investigator of the Laboratory of Computational Chemistry and Biochemistry (LCBC). She earned a bachelor degree in physical chemistry from the University of Bern, with the supervision of Prof. Ernst Schumacher. Her PhD work was completed in collaboration with the IBM Zürich Research Laboratory in Rüschlikon with Dr. Wanda Andreoni. Her postdoctoral work took place at the University of Pennsylvania in the group of Prof. Michael L. Klein and at the Max Planck Institute for Solid State Physics in the group of Prof. Michele Parrinello. She served as an assistant professor at ETH Zurich in computer-aided inorganic chemistry and as a visiting professor at SISSA in Italy. After moving to EPFL in 2002, she held the position of associate professor prior to becoming a full professor in 2009. From 2004-2007 she was also director of the Chemistry and Engineering Section. Her research interests are the development of multiscale computational methods and their applications to problems in biology and materials science.

1. Introduction

1.1 *DNA Oxidative Damage*

The human genome is under constant exposure to damage-inflicting endogenous and exogenous agents. The most common product of DNA harm, oxidative lesions, occur over 10,000 times per day in each cell.[1] If undetected and unrepaired, oxidative DNA defects promote further oxidation, point mutations, apurinic sites, or even strand breaks.[2,3] Accrued DNA injury has been implicated in oncogenesis, cancer progression, and neurodegenerative diseases,[4–8] which has triggered a deep interest in gaining a comprehensive, fundamental understanding of the origin of oxidative damage as well as its detection and repair.

The majority of oxidative damage to DNA occurs due to interaction of DNA with reactive oxygen species (ROS), which include molecular oxygen, hydroxyl radical, superoxide anion radical, hydrogen peroxide, and singlet oxygen. DNA exposure to ROS yields oxidized nucleobases with the most common being the 8-oxoguanine (8-oxoG) defect. Experimental and computational evidence confirm the low oxidation potential of guanine base in both gas and aqueous forms relative to other native bases, which explains the prevalence of guanine derivatives over other oxidative lesions in DNA such as 5-hydroxycytosine, 8-oxoadenine, and isoguanine amongst others (Fig. 1).[9–15]

Excessive ROS exposure in the cellular environment, especially when chronic, contributes to the onset and advancement of many diseases due to the increased quantity of oxidative DNA defects. While our cellular metabolic processes yield ROS natu-

**Correspondence:* Prof. U. Rothlisberger, E-mail: ursula.roethlisberger@epfl.ch, EPFL SB ISIC LCBC, CH-1015 Lausanne

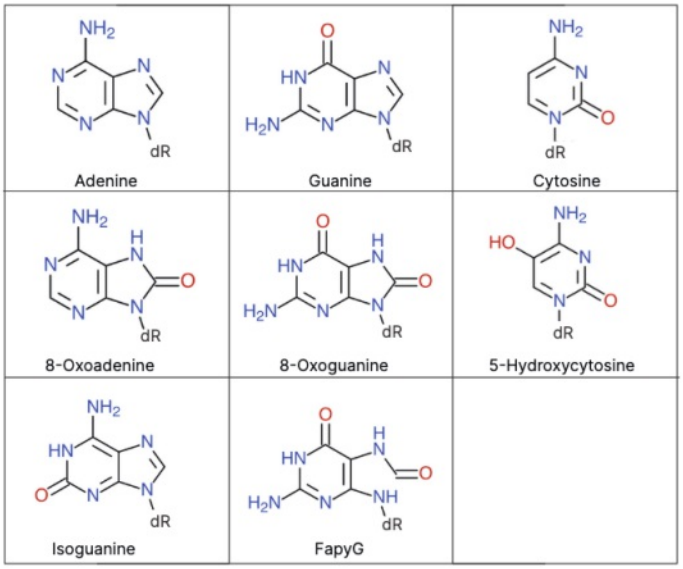

Fig. 1. Structural formulas of three native DNA bases (adenine, guanine, cytosine) with several of their common oxidative damage derivatives (8-oxoadenine, 8-oxogaunine, 5-hydroxycytosine, isoguanine and fapyG).

rally, behavioral and environmental factors – such as prolonged physical or psychological stress, smoking, UV radiation, and air pollution – promote further generation of and exposure to ROS.[16] Management of environmental factors can mitigate ROS impacts on our DNA only to a certain degree, yet developing efficacious therapeutics against oxidative damage requires a deeper knowledge of DNA repair.

Continuous research efforts produce valuable insights into the function of base excision repair enzymes (BERs), the central players of one of the major pathways involved in DNA repair. The type of damage dictates which BERs participate in the repair of small, non-bulky lesions such as 8-oxoguanine.[17] An oxidative lesion is initially excised by one of 11 human DNA glycosylases which leaves behind an apurinic site to be summarily patched by other BER enzymes.[17] BERs repair damage in both unpacked and packed (chromatin) forms of DNA. Unfortunately, repair rates of oxidative damage are reduced in the cellularly more abundant chromatin DNA structure likely as a consequence of the more complex network of electrostatic interactions and the diminished accessibility.[18–22] Strong DNA-protein interactions characterize the structural unit of chromatin, the nucleosome core particle (NCP), which contains a DNA helix of approximately 146 base pairs wrapped around a core of eight histone proteins.

In contrast to the rapidly emerging knowledge about the DNA repair process of BER enzymes and the development of promising anticancer therapeutics, *e.g.* those that block the function of key BERs leading to the accumulation of damage and accelerating cellular death,[23,24] much less is known about mechanisms for the continuous, efficacious scan of the large human genome which enables seemingly immediate detection of defects and signals damage type and location.

1.2 *Charge Transfer Model for DNA Damage Detection*

Despite the growing awareness of sources, impacts, and repair schemes of oxidative damage, the specific mechanisms of defect detection, especially in chromatin, remain an open question. Estimates suggest that a diffusive, base-by-base scanning process for damage detection by DNA glycosylases might not account for the rapid recognition of oxidative damaged lesions across the entire human genome.[25,26] Furthermore, oxidative damage products tend to incite small structural changes and can mimic native hydrogen bonding patterns.[27,28] In the face of such evidence, reliance on structural and mechanical attributes alone to flag defect bases appears inefficient. Alternatively, electrochemical processes have been invoked as the potential foundation for oxidative damage detection.

During the last 20 years, a charge transfer (CT) mechanism for DNA damage detection has increasingly garnered attention.[29–34] In this scheme, pairs of BER enzymes interrogate a stretch of DNA by dispatching a charge (usually a positive charge, *i.e.* a hole) between one another. In the case of an undamaged interconnecting DNA sequence, the second BER enzyme can receive the hole from its BER partner and unbind from the DNA helix to probe other locations. However, if the charge encounters a defect base with a lower oxidation potential than its native base, the hole becomes trapped. The BER enzyme which did not receive the now-trapped charge signal can stay on the helix to recruit other repair enzymes and to fine scan the involved DNA stretch to better locate the defect.

Examination of DNA glycosylases revealed that several contain 4Fe–4S clusters which could act as the donor and acceptor sites for CT across the DNA.[33,34] DNA conducts excess charge and holes effectively over long distances,[35,36] meaning a charge transfer process can occur at rate orders of magnitude faster than a base-by-base scanning process by a DNA glycosylase.

The CT transfer scheme for DNA defect detection relies on pronounced dissimilarities of redox free energies between native and defect bases so that the defect base can act as a reliable charge sink between two BERs. However, experimental evaluation of the redox free energy differences between such similar systems can be challenging or even impossible. Fortunately, modern computational chemistry techniques allow for accurate modeling of DNA at both classical and/or quantum mechanical levels of theory, *e.g.* within the framework of mixed quantum mechanical/molecular mechanical (QM/MM) simulations detailed in section 3 below.

2. Theoretical Basis to Study DNA Redox Properties

Computationalists and experimentalists alike frequently apply Warshel's vertical energy gap theory[37,38] together with Marcus' theory of electron transfer[39–42] to evaluate redox properties in biosystems from distributions of vertical ionization energies (VIEs) and vertical electron affinities (VEAs).[43–50] The description of this combined theoretical basis is abbreviated in this article, however, more detailed accounts of the underlying theory can be found in works by Sulpizi *et al.*,[46] Ghosh *et al.*,[43] Kılıç and Ensing,[47] and Diamantis *et al.*[49] amongst others. The vertical energy values represent the energy change when an electron is removed (respectively added) to the system at fixed nuclear positions. When a system undergoes a change in oxidation state *via* electron transfer (ET), its surrounding environment, including solvent, also 'reorganizes' thereby constituting an additional energetic contribution to the overall ET process. The ET rate reaches a maximum as the activation barrier for ET approaches zero, *i.e.* when the free energy needed for reorganization is balanced out by the gain in redox free energy. If an electron transfer process adheres to a linear solvent response, then resulting free energy curves for the two oxidation states of the system are intersecting parabolas along the reaction coordinate.

In fact, if the vertical energy distributions are Gaussian in shape and display negligible differences in variance (consistent with Marcus theory), then a simple relationship arises between the ensemble-averaged vertical energy values and the Helmholtz free energy of oxidation $\Delta A_{R\to O}$:

$$\Delta A_{R\to O} = \frac{\langle VIE\rangle + \langle VEA\rangle}{2} \quad (1)$$

where $\langle VIE \rangle$ and $\langle VEA \rangle$ respectively represent the ensemble averages of vertical energies arising from the reduced (VIE) and oxidized (VEA) states of the system.

Furthermore, the reorganization free energy (λ) of the redox reaction is also related to the ensemble averages of vertical energies, or alternatively, to the variance of the vertical energy distribution (σ), temperature (T), and the Boltzmann constant (k_B):

$$\lambda = \lambda_R = \lambda_O = \frac{\sigma^2}{2k_B T} = \frac{\langle VIE \rangle - \langle VEA \rangle}{2} \quad (2)$$

3. The QM/MM Approach

Only quantum mechanics (QM) properly captures electronic properties of a system (*e.g.* vertical energy values). However, a full QM treatment of a biosystem, such as a solvated nucleosome core particle with around 250,000 atoms, is computationally intractable. Further, carving out a small subsystem in isolation to describe with QM alone omits the crucial influence of the environment on structural and electronic properties. The impasse between computational resources and need for accurate modeling motivated development of the multiscale quantum mechanical/molecular mechanics (QM/MM) approach.[51–53]

In the QM/MM framework, the system Hamiltonian integrates three unique components: the quantum part (H_{QM}), the classical-part (H_{MM}), and the interaction between QM and MM parts of the system ($H_{QM\text{-}MM}$). Additive QM/MM schemes directly use such a composite Hamiltonian:

$$H_{tot} = H_{QM} + H_{MM} + H_{QM\text{-}MM} \quad (3)$$

Typically, H_{MM} is given by a classical (analytic) force field with established parameters to describe bond stretching, angle bending and torsions as well as parameters to describe the non-bonded van der Waals interactions and a (effective) point charge representation of the electrostatics. For H_{QM} on the other hand, a quantum chemical method is selected to approximately solve the time- independent many-electron electronic Schrödinger equation at a given nuclear configuration (Equation 4):

$$E_{elec}\Psi(r,R) = \hat{H}_{elec}\Psi(r,R) = [\hat{T}_e(r) + \hat{V}_{eN}(r,R) + \hat{V}_{NN}(R) + \hat{V}_{ee}(r)]\Psi(r,R) \quad (4)$$

Due to its favorable cost-accuracy ratio, Kohn-Sham Density Functional Theory (KS-DFT) is often the method of choice in first-principles based QM/MM simulations. DFT provides an exact solution to the ground state of the many-body quantum problem based on the electronic density $\rho(\boldsymbol{r})$, given the exchange-correlation functional $E_{xc}[\rho(\boldsymbol{r})]$ is known. Albeit, the exact $E_{xc}[\rho(\boldsymbol{r})]$ remains unknown, a hierarchy of accurate approximate exchange-correlation functionals has been developed during the years[54–56] enabling DFT based QM/MM simulations with accurate QM descriptions for extended systems and time scales.

Further, the interaction Hamiltonian $H_{QM\text{-}MM}$ incorporates both bonded and non-bonded contributions:

$$H_{QM\text{-}MM} = V_{QM\text{-}MM}^{bonded} + V_{QM\text{-}MM}^{nonbonded} \quad (5)$$

Bonded interactions between QM and MM atoms (including bond, angle, and torsional terms) are usually described at the level of the classical force field. However, for cases, in which the border between QM and MM parts transverses a chemical bond, special care has to be taken to saturate the open valence atoms in the QM description. Methods for this purpose include link atoms, monovalent pseudopotentials and more.[53] Non-bonded terms comprise van der Waals and electrostatic interactions. The former are usually treated at the classical level by assigning appropriate van der Waals parameters to the QM atoms. The latter are typically treated at the QM level with so-called electrostatic embedding, in which the electron density of the QM part is polarized by the electrostatic potential generated by the effective point charges of the MM surrounding. For the sake of computational efficiency, the electrostatic interactions between QM and MM subsystems often comprise a short-range contribution and a long-range contribution. The short-range term contains explicit Coulomb interactions between the QM and MM regions where the QM region is represented by the electron density at every point ($\boldsymbol{r}$) in space and the positive core charges situated at the QM nuclei while the MM part is represented by all effective point charges located at MM atoms. Longer range electrostatic interactions between QM and MM regions are instead described *via* a multipole expansion of the QM charge density.

In addition to purely static descriptions of a system, the QM/MM approach can also be combined with phase space sampling to generate ensemble averages of properties such as the vertical energies necessary to calculate $\Delta A_{R\to O}$ according to Equation 1. Typical sampling schemes follow either a Monte Carlo (MC) or a Molecular Dynamics (MD) approach, with the latter preferred for high-density biosystems. Classical time-propagation of a QM/MM system can be obtained using either Born-Oppenheimer dynamics (BOMD) or a Car-Parrinello scheme (CPMD).[57,58] Many software packages are currently available that offer a QM/MM option such as CPMD, CP2K, the flexible MiMiC framework, and more.[59–61]

4. Redox Properties of Native and Defect DNA Systems from QM/MM Simulations

In this section, selected studies of the 8-oxoguanine oxidative lesion in DNA illustrate the methods and theories previously discussed while providing insight into the impact of oxidative defects on DNA redox properties.

4.1 *Computational Setup*

The practical application of the QM/MM approach first requires a preparation and equilibration at the full MM level, *i.e.* with force field based MD for solvation, and thermalization of the systems at body temperature and atmospheric pressure. Classical MD packages such as Amber or GROMACS facilitate this preparation process.[62–64] Moving from a purely classical to a QM/MM model of a DNA system necessitates a suitable choice of the QM region. In the majority of examples below, three base pairs are included in the QM part with capping hydrogen atoms at the C5'–C4' and C3'–O3' bonds to ensure seamless QM-MM interfacing. With this choice of QM region, two base pairs flank a central guanine-cytosine base pair (native systems) or a central 8-oxoguanine-cytosine base pair (defect systems). A systematic study of the size effect for isolated quantum system of one and two base pairs was performed in ref. [65]. For the latter, the Gaussian 09 package[66] was utilized to apply DFT to static DNA fragment systems at the B3LYP/6-31++G* level.[67,68] For studies employing the QM/MM MD approach, the QM/MM-enabled version of CPMD 4.1[52,61,69–72] is the software of choice and the QM part is described using DFT at the BLYP level[55,56] with corresponding Dispersion-Corrected Atom-Centered Potentials (DCACPs) to account for dispersion forces.[73,74] Similar to classical equilibration, QM/MM simulations need NVT equilibration with BOMD or CPMD. Finally, a production run of NVE QM/MM MD, either 5 ps (unpacked DNA) or 25 ps (packed DNA), provides data for evaluation.

Both a free DNA system (unraveled DNA)[49] (Fig. 2A) and a solvated NCP system (packed/chromatin) (Fig. 2B) from recent work[50] will be discussed, as well as smaller units of DNA comprising between one to three base pairs. The related, recent publications provide further computational details for all systems reviewed.[49,50,65]

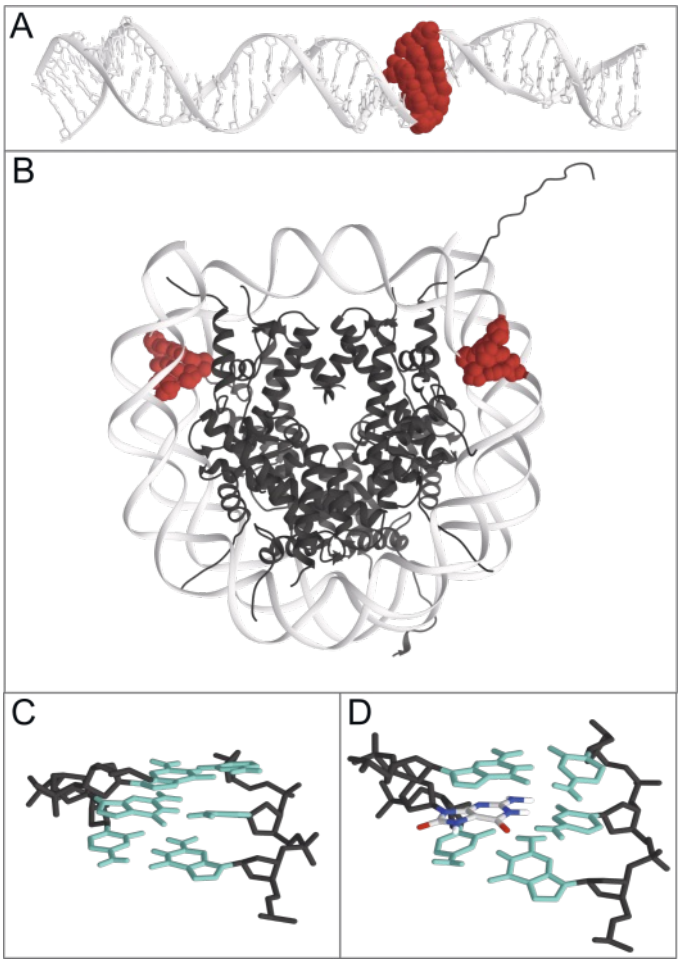

Fig. 2. **A**) Free double-helix DNA with 39 base pairs with the highlighted quantum region in red. The full solvated system includes approximately 50,000 atoms.[49] **B**) NCP DNA-protein complex (1AOI PDB)[75] with the two highlighted quantum regions in red (region 1 on left) and (region 2 on right).[50] The full solvated system includes approximately 252,500 atoms. Solvent and counter ions are not shown for the sake of clarity in **A**) and **B**). **C**) Illustrative quantum region containing three pairs of native bases in cyan. **D**) Illustrative quantum region containing three base pairs. Native bases are in cyan and the inserted 8-oxoG lesion is multicolored. In **C**) and **D**), the phosphate-sugar backbone atoms (black) are treated classically in QM/MM studies and explicitly in some parts of the fragment studies.[65]

4.2 *Redox Properties in Unpacked DNA*

As a precursor to QM/MM investigations, full QM approaches with and without a polarizable continuum model (PCM) have been used to study small DNA fragments (including one to three base pairs or one to two nucleotides as shown in Fig. 2C and 2D) in order to understand the effect of oxidative damage on DNA redox properties, *i.e.* vertical energies.[65] Both the gas phase and PCM results show VIE decreases as fragment size increases, though changes are more pronounced in the gas phase assessment indicating that solvent environment impacts redox properties of nucleic acids. Furthermore, fragments, such as those in Fig. 2C and 2D, containing an 8-oxoG lesion consistently show lower VIEs than their native counterparts, however only by up to -0.1 eV. Importantly, the study finds that convergence for VIE values as a function of fragment size is never attained for models of isolated DNA that are computationally feasible to study with full QM treatment. Furthermore, this study considered implicit solvent and DNA fragments in a static context, which excludes both the influence of a larger DNA environment and thermodynamic sampling of thermally relevant configurations.

Therefore, a follow-up QM/MM study applied the combined Marcus and Warshel approach with thermal sampling to evaluate differences not only in vertical energies, but also in redox free energies in extended DNA fragments (39-base pairs) with and without an 8-oxoG lesion. The study recovered the characteristic vertical energy distributions in good agreement with Marcus theory (Fig. 3). Values for the free energy of oxidation and the reorganization energy upon oxidation result from the analysis of between 400 and 600 snapshots along the 5 ps QM/MM MD simulation trajectory. The analysis shows that presence of the 8-oxoG lesion lowers the redox free energy by over 1.0 eV while the reorganization free energy changes by only 0.25 eV (see Table 1).[49,65] These values show a marked difference (10x greater) compared to the fragment-only studies emphasizing the need for models which take into account the short-range and long-range electrostatics in a solvated system, such as in QM/MM studies. Meanwhile, the differences in reorganization energies between native and defect systems are small relative to the larger difference in their free energies. Thus, while the energy required to adjust the environment to a new oxidation state is similar in both systems, the free energy change upon oxidation is substantially different for DNA containing a single 8-oxoG. Taken together, this evidence highlights the feasibility of a charge transfer mechanism of 8-oxoG lesion detection in unpacked DNA as 8-oxoG is more likely than native guanine to trap an incoming hole (positive charge) and halt the transfer of charge between BER enzymes.

4.3 *Redox Properties in Chromatin*

Electronic properties of DNA are highly sensitive to local environment.[76–79] Due to the strong DNA-protein interactions in chromatin, its electrostatics and structural properties vary greatly from those of free DNA.[80–82] However, an analogous evaluation of the redox properties of packed DNA as the one described above for free DNA, shows that the difference in redox free energies between native and defect containing systems persist also in packed DNA independent of defect location (region 1 and region 2 shown in Fig. 2B that differ in their solvent accessibility).[50] Table 2 displays ensemble averages for VIE and VEA along with calculated $\Delta A_{R\rightarrow O}$ and λ values for both studied regions of the NCP systems. Approximately 1000 frames from a 25 ps QM/MM MD simulation generated data for this study. As for free DNA, the distributions of VIE and VEA values are almost perfectly Gaussian for both regions generating characteristic parabolic Marcus curves. Differences in redox free energies between native and defect structures remain close to 1.0 eV while changes in reorganization energies are even less pronounced than for unpacked DNA. Meanwhile redox properties measured for the corresponding native systems remain similar across both regions. These observations strongly point to the viability of a charge transfer based detection mechanism for 8-oxoG lesions at any location within the genome. Disparity in rates of oxidative lesion repair between unpacked and packed DNA structures are thus likely due to the limited accessibility by BER enzymes involved in defect base removal and subsequent repair.

Well-equilibrated classical MD with subsequent QM/MM MD generates a wealth of thermally-sampled data, including structural properties for configurations visited by the system along the MD trajectories of defect-free and damaged DNA in their NCP packed forms. Therefore, in addition to the analysis of VIE and VEA,

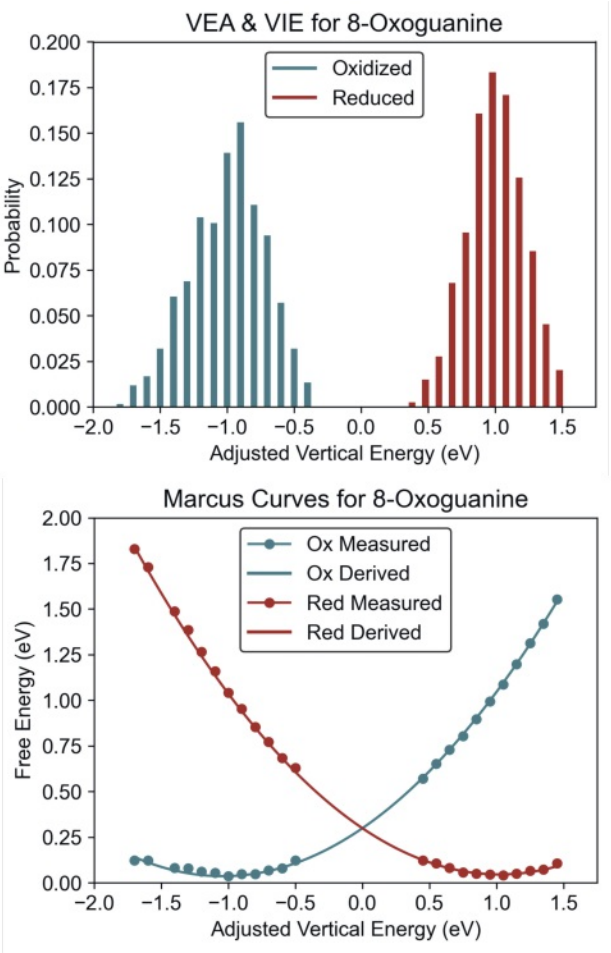

Fig. 3. Distributions of vertical energies for a free DNA system containing an 8-oxoG lesion (top) and corresponding Marcus curves (bottom).[49]

Table 1. Redox properties of unpacked DNA in its native form (Native) and containing an 8-oxoG defect (Defect). Data gathered *via* QM/MM MD simulations.[49]

Unpacked DNA		
Property	Native (eV)	Defect (eV)
$\langle VIE \rangle$	7.80 ± 0.22	6.62 ± 0.22
$\langle VEA \rangle$	5.30 ± 0.28	4.62 ± 0.28
$\Delta A_{R \to O}$	6.55 ± 0.28	5.62 ± 0.30
λ	1.25 ± 0.18	1.00 ± 0.18

41 unique geometric DNA parameters across configurations from 1 μs classical MD trajectories were evaluated with the CURVES+ software[83,84] to determine the possible degree of structural impact made by an 8-oxoG lesion. Fig. 4 compares the statistical distributions of some characteristic structural features sampled during the classical MD. As it is evident from Fig. 4, no significant changes between native and defect systems arise. The same holds for all analyzed parameters, indicating that the presence of 8-oxoG in chromatin generates no reliable structural indicators for defect detection.[50] As chromatin is the primary cellular form of human DNA, it appears essential that oxidative damage can be immediately detected even for DNA in its packed form. A lack of structural red flags for oxidative lesions strongly suggests that nature indeed relies on different properties, such as the change in redox free energies, to denote the presence of damage.

Table 2. Redox properties for two DNA systems representing packed (NCP) DNA structures. Data gathered *via* QM/MM MD simulations.[50]

NCP Region 1		
Property	Native (eV)	Defect (eV)
$\langle VIE \rangle$	7.82 ± 0.24	6.88 ± 0.23
$\langle VEA \rangle$	5.81 ± 0.24	4.59 ± 0.27
$\Delta A_{R \to O}$	6.81 ± 0.17	5.73 ± 0.18
λ	1.01 ± 0.17	1.14 ± 0.18
NCP Region 2		
Property	Native (eV)	Defect (eV)
$\langle VIE \rangle$	8.13 ± 0.24	6.93 ± 0.23
$\langle VEA \rangle$	5.77 ± 0.26	4.60 ± 0.27
$\Delta A_{R \to O}$	6.95 ± 0.18	5.77 ± 0.18
λ	1.18 ± 0.18	1.17 ± 0.18

5. Conclusion and Outlook

Hybrid integration of classical and quantum physics through a QM/MM framework allows for feasible computational modeling of systems at relevant biological temperature and solvation conditions. The QM/MM investigation into the impact of oxidative lesions on both structural and redox properties of packed DNA in conjunction with similar work on unpacked DNA demonstrate that the 8-oxoG oxidative lesion lowers the redox free energy by approximately 1.0 eV regardless of its location within unpacked DNA or chromatin structures. Furthermore, the stuies showcased indicate that the significance of redox changes are much more pronounced than DNA structural changes that are essentially absent (Fig. 4). Therefore, oxidative lesion detection based on electrochemical properties, as suggested by the proposed CT base detection mechanism, is likely more consistently reliable and universal than possible structural signals.

Two pathways for future work lie ahead: prediction of redox 'hotspots' in NCPs and modeling of a broad variety of different DNA damage types. MD simulations generate large amounts of data necessary to make observations, but the causes underlying the conclusions are not always obvious. Successful use of correlation-based feature selection combined with causal analysis, represents a powerful tool for dimensionality reduction and rationalization of observations in MD simulations.[85,86] Applying these approaches to QM/MM MD studies on DNA might establish casual criteria for chromatin systems sensitive to redox changes thereby leading to some predictive tool development for redox 'hotspots'. Additionally, other forms of DNA damage from Fig. 1 may affect redox and structural properties differently than 8-oxoG, especially those with a greater rearrangement of bonds from the native bases, such as the fapyG lesion, or large adducts such as those formed between hormone metabolites and DNA bases.

Acknowledgements

The authors gratefully acknowledge the Partnership for Advanced Computing in Europe (PRACE) for resources on JUWELS at the Jülich Supercomputing Centre in Germany (PRACE Project No. 2019204961). The authors also gratefully acknowledge the Swiss National Science Foundation for their generous funding (NSF Grants nos. 200020-185092, and 200020-219440). CSCS (project s1157) is also gratefully

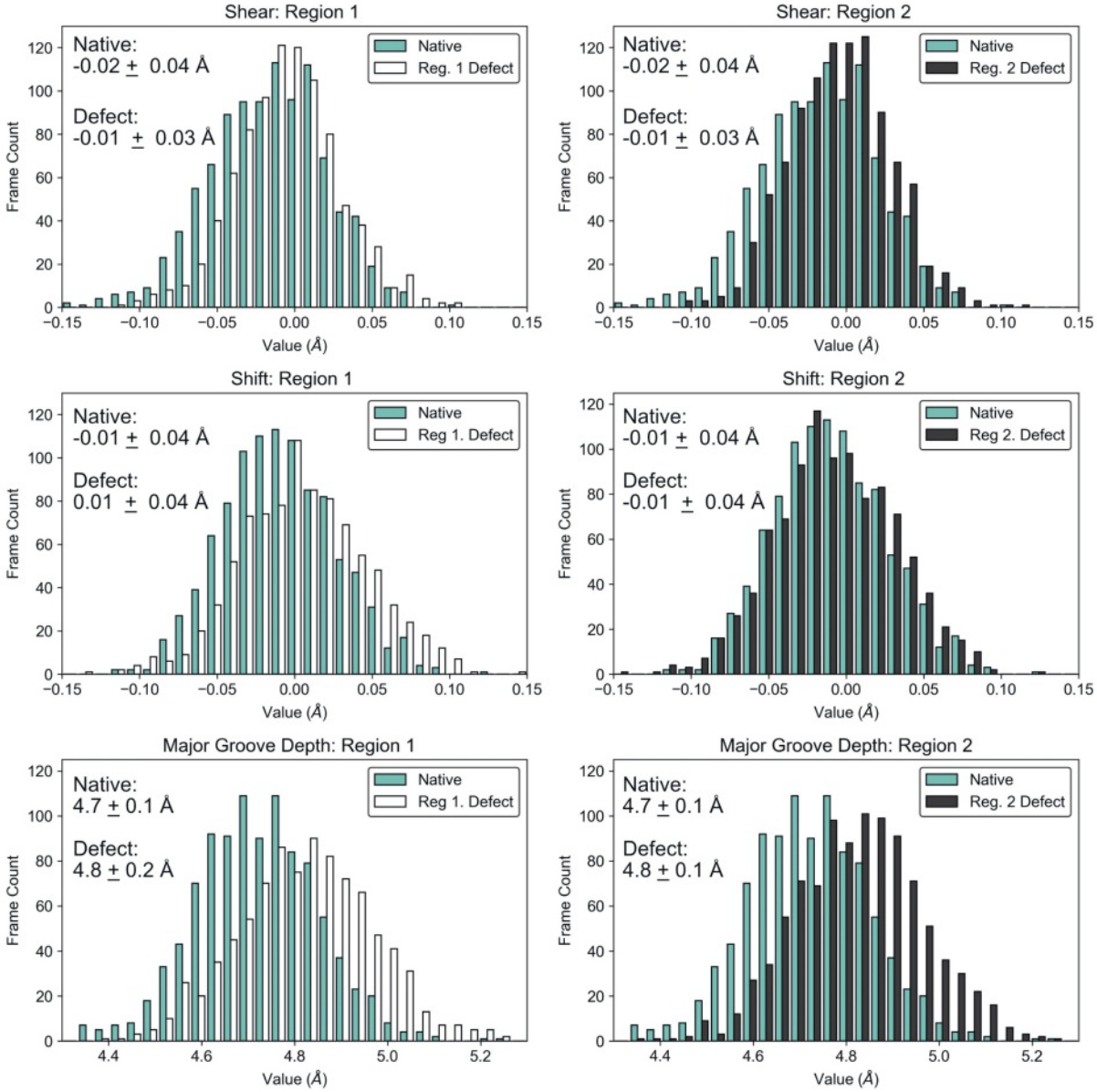

Fig. 4. Distributions of several illustrative structural features of DNA (shear, shift and major groove depth) from classical MD simulations indicate no significant differences in the structure of the DNA helices in a nucleosome core particle due to the presence of the 8-oxoG lesion located in region 1, respectively 2.[50]

acknowledged for computer time on the Piz Daint cluster. Finally, a special thanks is given to Polydefkis Diamantis, Ph.D., and Murat Kılıç, Ph.D., who designed all key studies reviewed in the results sections of this article. Their ingenuity and support are gratefully acknowledged.

Received: February 12, 2024

[1] B. N. Ames, M. K. Shigenaga, T. M. Hagen *Proc. Natl. Acad. Sci. U.S.A.* **1993**, *90*, 7915. https://doi.org/10.1073/pnas.90.17.7915
[2] T. B. Salmon, B. A. Evert, B. Song, P. W. Doetsch *Nucleic Acids Res.* **2004**, *32*, https://doi.org/10.1093/NAR/GKH696.
[3] A. R. Poetsch *CSBJ* **2020**, *18*, https://doi.org/10.1016/J.CSBJ.2019.12.013.
[4] S. P. Hussain, L. J. Hofseth, C. C. Harris *Nat. Rev. Cancer* **2003**, *3*, https://doi.org/10.1038/NRC1046.
[5] X. Chen, C. Guo, J. Kong *Neural Regen. Res.* **2012**, *7*, https://doi.org/10.3969/J.ISSN.1673-5374.2012.05.009.
[6] A. Tubbs, A. Nussenzweig *Cell* **2017**, *168*, 644, https://doi.org/10.1016/j.cell.2017.01.002.
[7] M. A. Lodato, R. E. Rodin, C. L. Bohrson, M. E. Coulter, A. R. Barton, M. Kwon, M. A. Sherman, C. M. Vitzthum, L. J. Luquette, C. N. Yandava, P., Yang, T. W. Chittenden, N. E. Hatem, M. B. Woodworth P. J. Park, C. A. Walsh, *Science* **2018**, *359*, 555, https://doi.org/10.1126/science.aao4426.
[8] E. C. Cheung, K. H. Vousden *Nat. Rev. Cancer* **2022**, *22*, 280, https://doi.org/10.1038/s41568-021-00435-0.
[9] N. S. Hush, A. S. Cheung *Chem. Phys. Lett.* **1975**, *34*, 11, https://doi.org/10.1016/0009-2614(75)80190-4.
[10] M. S. Cooke, M. D. Evans, M. Dizdaroglu, J. Lunec *FASEB* **2003**, *17*, https://doi.org/10.1096/FJ.02-0752REV.
[11] S. Fukuzumi, H. Miyao, K. Ohkubo, T. Suenobu *J. Phys. Chem. A* **2005**, *109*, https://doi.org/10.1021/JP0459763.
[12] Y. Paukku, G. Hill *J. Phys. Chem. A* **2011**, *115*, 4804, https://doi.org/10.1021/jp201281t.
[13] E. Pluharova, P. Jungwirth, S. E. Bradforth, P. Slavicek *J. Phys. Chem. B* **2011**, *115*(5), 1294, https://doi.org/10.1021/jp110388v.
[14] C. A. Seidel, A. Schulz, M. H. Sauer *J. Phys. Chem.* **1996**, *100*, 5541, https://doi.org/10.1021/jp951507c.
[15] A. Heller *Faraday Discuss.* **2000**, *116*, 1, https://doi.org/10.1039/b006196o.
[16] D. Ziech, R. Franco, A. G. Georgakilas, S. Georgakila, V. Malamou-Mitsi, O. J. L. M. Schoneveld, A. Pappa, M. I. Panayiotidis, M. I. Panayiotidis *Chem.-Biol. Interact.* **2010**, *188*, https://doi.org/10.1016/J.CBI.2010.07.010.
[17] E. Markkanen *DNA Repair* **2017**, *59*, https://doi.org/10.1016/J.DNAREP.2017.09.007.
[18] P. C. Blainey, A. M. van Oijen, A. Banerjee, G. L. Verdine, X. S. Xie *Proc. Natl. Acad. Sci. U.S.A* **2006**, *103*, https://doi.org/10.1073/PNAS.0509723103.
[19] J. I. Friedman, J. T. Stivers *Biochemistry* **2010**, *49*, https://doi.org/10.1021/BI100593A.

[20] B. C. Beard, S. H. Wilson, M. J. Smerdon *Proc. Natl. Acad. Sci. U.S.A* **2003**, *100*, https://doi.org/10.1073/PNAS.1330328100.

[21] I. D. Odell, K. Newick, N. H. Heintz, S. S. Wallace, D. S. Pederson *DNA Repair* **2010**, *9*, https://doi.org/10.1016/J.DNAREP.2009.11.005.

[22] R. L. Maher, A. Prasad, O. Rizvanova, S. S. Wallace, D. S. Pederson *DNA Repair* **2013**, *12*, https://doi.org/10.1016/J.DNAREP.2013.08.010.

[23] S. Neijenhuis, A. C. Begg, C. Vens *Radiother. Oncol.* **2005**, *76*, https://doi.org/10.1016/J.RADONC.2005.06.020.

[24] X. Gao, J. Wang, M. Li, J. Wang, J. Lv, L. Zhang, C. Sun, J. Ji, W. Yang, Z. Zhao, W. Mao *J. Cell. Mol. Med.* **2019**, *23*, https://doi.org/10.1111/JCMM.14560.

[25] J. T. Stivers, Y. L. Jiang *Chem. Rev.* **2003**, *103*, https://doi.org/10.1021/CR010219B.

[26] K. A. Eriksen *Theor. Biol. Med. Model.* **2005**, *15*, https://doi.org/10.1186/1742-4682-2-15.

[27] B. van Loon, E. Markkanen, U. Hübscher *DNA Repair* **2010**, *9*(6), 604, https://doi.org/10.1016/j.dnarep.2010.03.004.

[28] W. A. Beard, V. K. Batra, S. H. Wilson, *Mutat. Res. Genet. Toxicol. Environ. Mutagen.* **2010**, *703*, 18, https://doi.org/10.1016/j.mrgentox.2010.07.013.

[29] E. Yavin, A. K. Boal, E. D. A. Stemp, E. M. Boon, A. L. Livingston, V. L. O'Shea, S. S. David, J. K. Barton *Proc. Natl. Acad. Sci. U.S.A* **2005**, *102*, 3546, https://doi.org/10.1073/PNAS.0409410102.

[30] A. K. Boal, J. C. Genereux, P. A. Sontz, J. A. Gralnick, D. K. Newman, J. K. Barton *Proc. Natl. Acad. Sci. U.S.A* **2009**, *106*, 15237, https://doi.org/10.1073/PNAS. 0908059106.

[31] J. C. Genereux, A. K. Boal, J. K. Barton *J. Am. Chem. Soc.* **2010**, *132*, 891, https://doi.org/10.1021/JA907669C.

[32] P. A. Sontz, N. B. Muren, J. K. Barton *Acc. Chem. Res.* **2012**, *45*, https://doi.org/10.1021/AR3001298.

[33] M. A. Grodick, H. M. Segal, T. J. Zwang, J. K. Barton *J. Am. Chem. Soc.* **2014**, *136*, https://doi.org/10.1021/JA501973C.

[34] E. O'Brien, R. M. Silva, J. K. Barton *Isr. J. Chem.* **2016**, *56*, https://doi.org/10.1002/IJCH.201600022.

[35] M. E. Núñez, D. B. Hall, J. K. Barton *Chemistry & Biology* **1999**, *6*, https://doi.org/10.1016/S1074-5521(99)80005-2.

[36] M. E. Núñez, G. P. Holmquist, J. K. Barton *Biochemistry* **2001**, *40*, https://doi.org/10.1021/ BI011560T.

[37] A. Warshel *J. Phys. Chem.* **1982**, *86*, 2218, https://doi.org/10.1021/j100209a016.

[38] G. King, A. Warshel *J. Chem. Phys.* **1990**, *93*, 8682, https://doi.org/10.1063/1.459255.

[39] R. A. Marcus *J. Chem. Phys.* **1956**, *24*, 979, https://doi.org/10.1063/1.1742724.

[40] R. A. Marcus *J. Chem. Phys.* **1956**, *24*, 966, https://doi.org/10.1063/1.1742723.

[41] R. A. Marcus *J. Chem. Phys.* **1957**, *26*, 872, https://doi.org/10.1063/1.1743424.

[42] R. A. Marcus *J. Chem. Phys.* **1965**, *43*, 679, https://doi.org/10.1063/1.1696792.

[43] D. Ghosh, A. Roy, R. Seidel, B. Winter, S. E. Bradforth, A. I. Krylov *J. Phys. Chem. B* **2012**, *116*, https://doi.org/10.1021/JP301925K.

[44] M. Cascella, A. Magistrato, I. Tavernelli, P. Carloni, U. Rothlisberger *Proc. Natl. Acad. Sci. U.S.A* **2006**, *103*, 19641, https://doi.org/10.1073/pnas.0607890103.

[45] J. VandeVondele, M. Sulpizi, M. Sprik *Angew. Chem. Int. Ed.* **2006**, *45*, https://doi.org/10.1002/ANIE.200503581.

[46] M. Sulpizi, S. Raugei, J. VandeVondele, P. Carloni, M. Sprik *J. Phys. Chem. B* **2007**, *111*, 3969, https://doi.org/10.1021/jp067387y.

[47] M. Kılıç, B. Ensing *J. Chem. Theory Comput.* **2013**, *9*, 3889, https://doi.org/10.1021/ct400088g.

[48] T. Firmino, E. Mangaud, F. Cailliez, A. Devolder, D. Mendive-Tapia, F. Gatti, C. Meier, M. Desouter-Lecomte, A. De La Lande *Phys. Chem. Chem. Phys.* **2016**, *18*, 21442, https://doi.org/10.1039/C6CP02809H.

[49] P. Diamantis, I. Tavernelli, U. Rothlisberger *J. Chem. Theory Comput.* **2020**, *16*, 6690, https://doi.org/10.1021/acs.jctc.0c00568.

[50] M. Kılıç, P. Diamantis, S. K. Johnson, O. Toth, U. Rothlisberger *J. Chem. Theory Comput.* **2023**, *19*, 8434, https://doi.org/10.1021%2Facs.jctc.3c01013.

[51] A. Warshel, M. Levitt *J. Mol. Biol.* **1976**, *103*, 227, https://doi.org/10.1016/0022-2836(76)90311-9.

[52] E. Brunk, U. Rothlisberger *Chem. Rev.* **2015**, *115*, 6217, https://doi.org/10.1021/cr500628b.

[53] G. Groenhof *Methods Mol. Biol.* **2013**, *924*, 43, https://doi.org/10.1007/978-1-62703-017-5_3.

[54] N. Mardirossian, M. Head-Gordon *Mol. Phys.* **2017**, *115*, 2315, https://doi.org/10.1080/00268976.2017.1333644.

[55] A. D. Becke *Phys. Rev. A: At., Mol., Opt. Phys.* **1988**, *38*, 3098, https://doi.org/10.1103/PhysRevA.38.3098.

[56] C. Lee, W. Yang, R. G. Parr *Phys. Rev. B: Condens. Matter Mater. Phys.* **1988**, *37*, 785, https://doi.org/10.1103/physrevb.37.785.

[57] M. Born, R. Oppenheimer *Annalen der Physik* **1927**, *389*, 457, https://doi.org/10.1002/andp.19273892002.

[58] R. Car, M. Parrinello *Phys. Rev. Lett.* **1985**, *55*, 2471, https://doi.org/10.1103/PhysRevLett.55.2471.

[59] T. D. Kühne, M. Iannuzzi, M. Del Ben, V. V. Rybkin, P. Seewald, F. Stein, T. Laino, R. Z. Khaliullin, O. Schütt, F. Schiffmann, D. Golze, J. Wilhelm, S. Chulkov, M. H. Bani-Hashemian, V. Weber, U. Borštnik, M. Taillefumier, A. S. Jakobovits, A. Lazzaro, H. Pabst, T. Müller, R. Schade, M. Guidon, S. Andermatt, N. Holmberg, G. K. Schenter, A. Hehn, A. Bussy, F. Belleflamme, G. Tabacchi, A. Glöß, M. Lass, I. Bethune, C. J. Mundy, C. Plessl, M. Watkins, J. VandeVondele, M. Krack, J. Hutter *J. Chem. Phys.* **2020**, *152*, https://doi.org/10.1063/5.0007045.

[60] J. M. H. Olsen, V. Bolnykh, S. Meloni, E. Ippoliti, M. P. Bircher, P. Carloni, U. Rothlisberger *J. Chem. Theory Comput.* **2019**, *15*, 3810, https://doi.org/10.1021/acs.jctc.9b00093.

[61] The CPMD Consortium Page, **2019**. The CPMD program is © 2000–2019 jointly by IBM Corp. and by Max Planck Institute, Stuttgart. It is distributed free of charge to non-profit Organizations under the CPMD free licence. http: //www.cpmd.org, 2019.

[62] D. A. Case, H. M. Aktulga, K. Belfon, D. S. Cerutti, G. A. Cisneros, V. W. D. Cru eiro, N. Forouzesh, T. J. Giese, A. W. Götz, H. Gohlke, S. Izadi, K. Kasavajhala, M. Kaymak, E. King, T. Kurtzman, T.-S. Lee, P. Li, J. Liu, T. Luchko, R. Luo, M. Manathunga, M. R. Machado, H. M. Nguyen, K. A. O'Hearn, A. V. Onufriev, F. Pan, S. Pantano, R. Qi, A. Rahnamoun, A. Risheh, S. Schott-Verdugo, A. Shajan, J. Swails, J. Wang, H. Wei, X. Wu, Y. Wu, S. Zhang, S. Zhao, Q. Zhu, T. E. Cheatham III, D. R. Roe, A. Roitberg, C. Simmerling, D. M. York, M. C. Nagan, K. M. Merz Jr. *J. Chem. Inf. Model.* **2023**, *63*, 6183, https://doi.org/10.1021/acs.jcim.3c01153.

[63] M. J. Abraham, T. Murtola, R. Schulz, S. Páll, J. C. Smith, B. Hess, E. Lindahl *SoftwareX* **2015**, *1–2*, 19, https://doi.org/10.1016/j.softx.2015.06.001.

[64] S. Páll, M. J. Abraham, C. Kutzner, B. Hess, E. Lindahl, Tackling exascale software challenges in molecular dynamics simulations with GROMACS ; Springer International Publishing Switzerland, London: **2015**, pp 3–27.

[65] P. Diamantis, I. Tavernelli, U. Rothlisberger *J. Chem. Theory Comput.* **2019**, *15*, 2042, https://doi.org/10.1021/acs.jctc.8b00645.

[66] M. J. Frisch, G. W. Trucks, H. B. Schlegel, G. E. Scuseria, M. A. Robb, J. R. Cheeseman, G. Scalmani, V. Barone, G. A. Petersson, H. Nakatsuji, X. Li, M. Caricato, A. Marenich, J. Bloino, B. G. Janesko, R. Gomperts, B. Mennucci, H. P. Hratchian, J. V. Ortiz, A. F. Izmaylov, J. L. Sonnenberg, D. Williams-Young, F. Ding, F. Lipparini, F. Egidi, J. Goings, B. Peng, A. Petrone, T. Henderson, D. Ranasinghe, V. G. Zakrzewski, J. Gao, N. Rega, G. Zheng, W. Liang, M. Hada, M. Ehara, K. Toyota, R. Fukuda, J. Hasegawa, M. Ishida, T. Nakajima, Y. Honda, O. Kitao, H. Nakai, T. Vreven, K. Throssell, J. A. Montgomery Jr., J. E. Peralta, F. Ogliaro, M. Bearpark, J. J. Heyd, E. Brothers, K. N. Kudin, V. N. Staroverov, T. Keith, R. Kobayashi, J. Normand, K. Raghavachari, A. Rendell, J. C. Burant, S. S. Iyengar, J. Tomasi, M. Cossi, J. M. Millam, M. Klene, C. Adamo, R. Cammi, J. W. Ochterski, R. L. Martin, K. Morokuma, O. Farkas, J. B. Foresman, D. J. Fox, *Gaussian 09, Revision A.1; Gaussian, Inc., Wallingford CT*: **2009**.

[67] C. Lee, W. Yang, R. G. Parr *Phys. Rev. B: Condens. Matter Mater. Phys.* **1988**, *37*, 785, https://doi.org/10.1103/physrevb.37.785.

[68] A. D. Becke *J. Chem. Phys.* **1993**, *98*, 5648, https://doi.org/10.1063/1.464913.

[69] A. Laio, J. VandeVondele, U. Rothlisberger *J. Chem. Phys.* **2002**, *116*, 6941, https://doi.org/10.1063/1.1462041.

[70] M. C. Colombo, L. Guidoni, A. Laio, A. Magistrato, P. Maurer, S. Piana, U. Röhrig, K. Spiegel, M. Sulpizi, J. VandeVondele, M. Zumstein, U. Rothlisberger *CHIMIA* **2002**, *56*, 13, https://doi.org/10.2533/000942902777680865.

[71] W. F. van Gunsteren, H. J. C. Berendsen, 'Molecular Simulation [GROMOS] Library Manual'; Biomos, Groningen, The Netherlands: **1987**, pp 1–221.

[72] W. F. van Gunsteren, S. R. Billeter, A. A. Eising, P. H. Hünenberger, P. Krüger, A. E. Mark, W. R. P. Scott, I. G. Tironi, 'Biomolecular Simulation: The GROMOS96 Manual and User Guide'; Vdf Hochschulverlag AG an der ETH Zürich, Zürich, Switzerland: **1996**, pp 1–1042.

[73] O. A. von Lilienfeld, I. Tavernelli, U. Rothlisberger, D. Sebastiani *Phys. Rev. Lett.* **2004**, *93*, 153004, https://doi.org/10.1103/PhysRevLett.93.153004.

[74] I.-C. Lin, M. D. Coutinho-Neto, C. Felsenheimer, O. A. von Lilienfeld, I. Tavernelli, U. Rothlisberger *Phys. Rev. B* **2007**, *75*, 205131, https://doi.org/10.1103/PhysRevB.75.205131.

[75] K. Luger, A. W. Mäder, R. K. Richmond, D. F. Sargent, T. J. Richmond *Nature* **1997**, *389*, 251, https://doi.org/10.1038/38444.

[76] I. Saito, T. Nakamura, K. Nakatani, Y. Yoshioka, K. Yamaguchi, H. Sugiyama *J. Am. Chem. Soc.* **1998**, *120*, 12686, https://doi.org/10.1021/ja981888i.

[77] X. Li, Y. Peng, J. Ren, X. Qu *Biochemistry* **2006**, *45*, 13543, https://doi.org/10.1021/bi061103i.

[78] D. W. Small, D. V. Matyushov, G. A. Voth *J. Am. Chem. Soc.* **2003**, *125*, 7470, https://doi.org/10.1021/ja029595j.

[79] E. Cauet, M. Valiev, J. H. Weare *J. Phys. Chem. B* **2010**, *114*, 5886, https://doi.org/10.1021/jp9120723.

[80] C. Davey, D. Sargent, K. Luger, A. Maeder, T. Richmond *J. Mol. Biol.* **2002**, *319*, 1097, https://doi.org/10.1016/s0022-2836(02)00386-8.

[81] J. Widom *Annu. Rev. Biophys. Biomol. Struct.* **1998**, *27*, 285, https://doi.org/10.1146/annurev.biophys.27.1.285.

[82] A. Wolffe, Chromatin Structure and Function; San Diego Academic Press, Inc.: **1992**.
[83] R. Lavery, M. Moakher, J. H. Maddocks, D. Petkeviciute, K. Zakrzewska *Nucleic Acids Res.* **2009**, *37*, 5917, https://doi.org/10.1093/nar/gkp608.
[84] C. Blanchet, M. Pasi, K. Zakrzewska, R. Lavery *Nucleic Acids Res* **2011**, *39*, W68, https://doi.org/10.1093/nar/gkr316.
[85] P. Campomanes, M. Neri, B. A. C. Horta, U. F. Röhrig, S. Vanni, I. Tavernelli, U. Rothlisberger *J. Am. Chem. Soc.* **2014**, *136*, https://doi.org/10.1021/JA411303V.
[86] S. C. van Keulen, A. Solano, U. Rothlisberger *J. Chem. Theory Comput.* **2017**, *13*, 4524, https://doi.org/10.1021/ACS.JCTC.7B00229.

License and Terms

The definitive version of this article is the electronic one that can be found at https://doi.org/10.2533/chimia.2024.243